ROTATING SCATTER MASK FOR NEUTRON SOURCE IMAGING

Nicholas Quartemont

Abstract—**Rotating scattering masks offer a method to characterize radiation sources when coupled with a radiation detector which is beneficial for the broad scientific community to locate and track unknown radiation sources. A rotating scattering mass is a material with complex geometry placed over a detector to increase the linear independence of the solutions. The objective was to use a gamma radiation mask setup and translate it to detect and locate neutron sources. The monte-carlo transport code, MCNP6.14, was used to create detector energy dependent response functions. The detector response was compared in 72 source positions for 500 keV, 2 MeV, and 14.1 MeV source neutrons with a mask composed of a lead-bismuth eutectic and a high-density polyethylene. The energy depended response functions shown strong linear relationship of 0.99 +/- 0.02, which minimizes the direction detectability of source neutrons in short timescales. The integrated response function displays more uniqueness in the detectability; however, more measurement time is required to characterize the source. The uniqueness of the detector responses indicates that the entire mask response is required to determine a solution for the source position.**

Index Terms—**neutron, detection, scattering, imaging, mask, nuclear**

I. INTRODUCTION

NEUTRON measurement and detection is important for an array of applications of interest to the Department of Defense and the scientific community in general. Notable applications of neutron detection are nuclear non-proliferation monitoring, nuclear materials security and search, and weapons detection. A robust capability enables the source to be characterized and located.

The Air Force Institute of Technology (AFIT) has demonstrated rotating scattering masks (RSMs) capability to provide a means of determining the location of a gamma radiation source. The RSM is used in conjunction with a detector to provide a source location on the order of an hour. The RSM application can also be extended to a degree for neutron sources. Energy deposition differs between gammas and neutrons in materials, which creates a major challenge for this project. Gamma radiation deposits energy in relatively fine peaks, while neutron radiation creates a spectrum of responses from a detector.
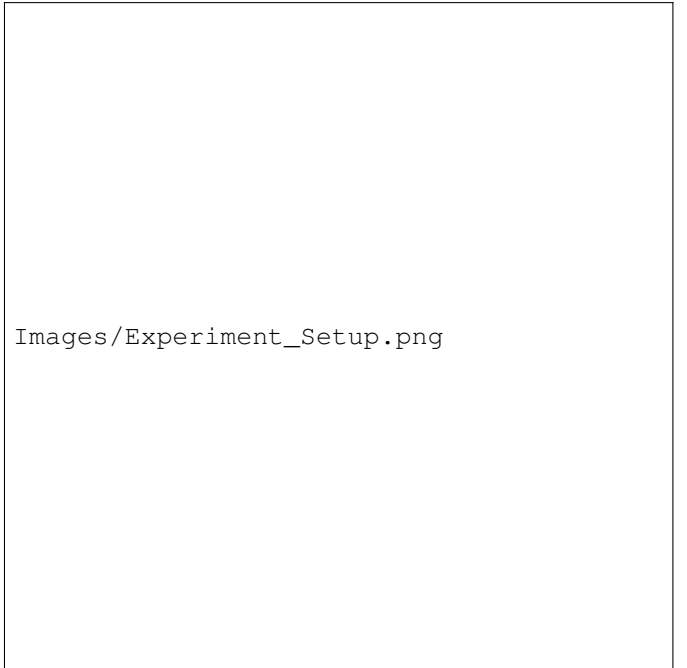
This work aims to modify the gamma RSM model with a neutron source to provide a first-look at the uniqueness of the detector responses, with a focus on linearly independent solutions to decrease the time to orient the direction to the radiation source. Important aspects of neutron detection modeled and varied in conjunction with the RSM include neutron energy, source direction, and RSM material. The detector response for each variation can be analyzed. A large variance in the response of a detector allows for low degeneracy in the solution for source location. The uniqueness of the detector responses will be represented by the dot product of two response matrices divided by the product of magnitudes of each matrix.

II. PROBLEM DESCRIPTION

The RSM is modeled with varying neutron energy, source position, and RSM material. The scope of the project is limited to 0.5, 2, and 14.1 MeV neutrons using the existing RSM geometry with a 2" EJ-309 detector. The source location is placed at 72 points. The RSM is modeled with two materials: a high-density polyethylene (HDPE) and a Lead-Bismuth eutectic (LBE). The results to be presented show the energy deposited in the detector as a function of energy, which is linked to the uniqueness of the response functions. The scope determined allows for a top level view of the feasibility of extending the RSM to neutron sources.

The 72 source locations are 86.36 cm from the detector with an azimuthal angle ϕ of 45 degrees. The experimental setup is shown in Figure **??** [**?**]. Each angle tested is at five degree increments in the horizontal plane, completing a full 2π rotation around the azimuthal angle. The rotation characterizes a slice of the response from the whole RSM.

Fig. 1. Experimental Setup.

The uniqueness of the response functions is determined with a model assurance criterion (MAC) as shown in equation

??. The MAC represents the relationship between two vectors, which will be unity if there is a strong linear relationship and zero to indicate linear independence [**?**]. The MAC between two responses is a function of the magnitude of the detector counts and the energy spectrum of the counts. The MAC is determined for each neutron source energy and RSM material. A matrix of MACs can be formed to show the general uniqueness of the RSM with angular dependence. The error is the MAC is taken as the square root of the quadrature sum of the errors in the underlying distribution.

$$MAC = (\frac{\mathbf{A} \cdot \mathbf{B}}{|\mathbf{A}||\mathbf{B}|})^2 \qquad (1)$$

The mix of neutron energy, source location, and RSM material provides a comprehensive first look analysis of the uniqueness of the detector responses. The neutron energy source was chosen to test neutrons at low energy that are still detectable with an EJ-309, fission energy, and fusion energy. The neutrons interact with the RSM material and scatter or pass through, to the detector. The LBE and HDPE materials offer two very different options for neutron interaction. LBE is composed of high atomic mass isotopes, so the average neutron energy loss is very low. HDPE is composed of a low mass organic compounds, so more thermalization of the neutrons occurs.

III. Description of Work

The process to build and analyze the neutron RSM involved MCNP Version 6.14 and Python 2.7. MCNP was used for the model, neutron transport calculations, and detector response. Post-processing of the data from MCNP utilized Python. MCNP created a large number of output files, 72 for each setup. Python's features allow for an expedited process of evaluating the entire dataset.

The MCNP model used for the RSM was adapted from a collection of MCNP6.14 scripts for the gamma RSM work conducted at AFIT [**?**]. The key modifications made to the MCNP script include the MCNP geometry, RSM materials, source definition, and detector tally.

The 2" EJ-309 detector employed a model from an external Github Repository from Slaybaugh Lab [**?**]. The EJ-309 required a modification to fit inside of the RSM, which involved external interfaces, such as mounts and flanges to be removed. The EJ-309 is 2" in diameter.

The detector response in MCNP utilized the F8 tally built-in, which counts the energy distribution of pulses in a detector [**?**]. The energy distribution is created from an energy balance from the events in the simulation. The neutron energies are cutoff at 250 keV, which is a typical threshold value to cause scintillation in an EJ-309 detector. The F8 tally utilizes two catch energy bins to remove counts that do not transfer to a physical pulse count. These catch bins occur at 0 eV and 1 eV. The catch bins are necessary despite the energy cutoff because the neutrons can still impart energies below 250 keV to the detector.

The tally chosen is an area of potential error in the results. The F8 tally sets a warning message when an F8 tally

is utilized with neutrons, as the results may be unreliable. The Los Alamos National Laboratory manual for MCNP6 cites that the correct pulses for the F8 tally are extremely limited [**?**]. Neutrons may not work as expected because of their non-analog physics, which is more complex than gamma interactions with material [**?**].

The gamma RSM model was generally left intact for the neutron source modifications. The neutron cross-section libraries were changed to the neutron form. The source definition was modified to emit neutrons instead of gammas. The LBE was modeled at 44.5 weight percent lead and 55.5 weight percent bismuth with a density of $10.756 g/cm^3$ [**?**].

The geometry of the MCNP model is shown in Figure **??**. The shape of the RSM is not readily apparent in this form. The mask is a surface of varying thicknesses. The plane at a height of 10 centimeters is important for analysis as it is in-line with the source direction to the detector. The MCNP files require MCNP Version 6.14 to utilize the unstructured mesh that defines the RSM geometry. The RSM geometry utilized is the the same as the original work.

`Images/All.png`

Fig. 2. MCNP Geometry.

The MCNP input utilized the ENDF/B-VI nuclear data files at room temperature. The number of source particles for each run is 10,000,000. On 16 cores, the 72 simulations over the six configurations can be accomplished in approximately one day.

The post-processing analysis centers around flexibility and repeatability to optimize the turnaround of output information to changes in the project. A prompt return of output is essential to parse through the six configurations of 72 MCNP output files.

A MCNP 6.14 tally reading output function in Python automates the process of importing data into a structured array for post-processing. The tally reading function is adapted from

a Github Repository from Nuclear Engineering 685 at AFIT [**?**]. The tally reading function is coupled with a file searching function to search through the output files and extract the tally information. The MCNP inputs and post-processing functions are available on a Github Repository [**?**].

IV. RESULTS

The detector response, detector response functions, and MAC value aspects of the results highlight the deficiency in the RSM setup to image a neutron source. The detector response shows the energy dependent pulse count for a tally. The neutron response function is the integrated detector response. The MAC values show the uniqueness of the response function.

A. Detector Responses

The detector responses are shown for the LBE tally results. Overall, there are a few aspects of the response functions that are not physical. It is highly likely that this area requires further work to determine a new tally to produce the correct results. The remainder of the analysis is carried out to aid in future studies. The plots are done with errorbars.

The expected results for this section is an increases in energy deposition tallies as the energy is decreased. The peak value should occur at low energies. The mechanism for energy deposition for neutrons in detectors is elastic and inelastic scattering. Based on the angle of the scatter, the neutron will deposit a fraction of its energy to the detector.

The results of the 14.1 MeV neutron source MCNP simulation detector responses with the F8 tally are shown in Figure **?** for the LBE RSM. The detector response curves follow the same shape the HDPE RSM at 14.1 MeV.

Images/FluxLBE14MeV.png

Fig. 3. Detector Response Energy Spectrum for 14.1 MeV Neutrons in LBE RSM.

The energy dependent pulse count shape is characterized by a large region of nearly constant energy deposition at low levels. The pulse counts of energy deposition increases at lower energies, which is consistent with expectations.

There is an increase in energy deposition at the source energy that is not physical. The increase implies that there is a preference for the neutron to deposit its full energy when interacting with the detector. An important note here is that the shape of the detector responses is nearly the same with an increase in magnitude based on the direction. The result of similar detector responses indicates that there is a strong linear correlation between the data sets, so the MAC is low for this slice of the RSM.

The results of the 2 MeV neutron source MCNP simulation detector responses with the F8 tally are shown in Figure **?** for the LBE RSM. The detector response curves follow the same shape the HDPE RSM at 2 MeV.
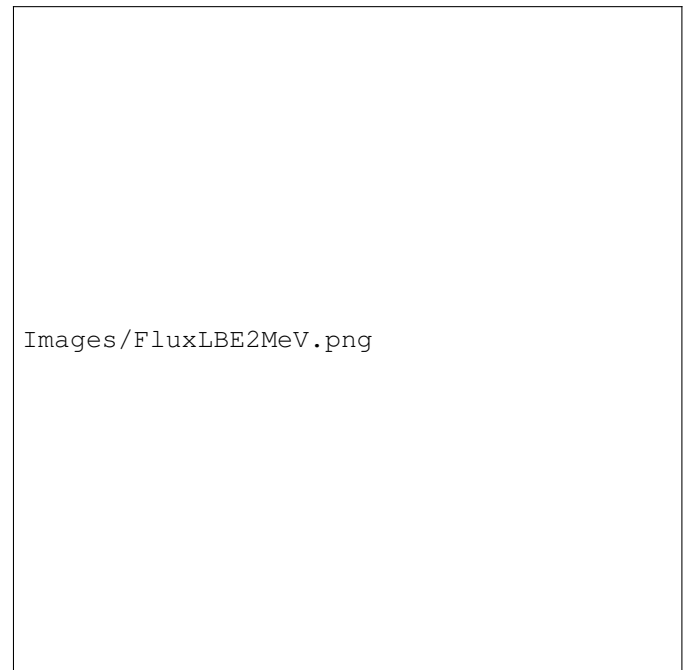
Images/FluxLBE2MeV.png

Fig. 4. Detector Response Energy Spectrum for 2 MeV Neutrons in LBE RSM.

The 2 MeV detector response are also not what is expected. Again, there is a large peak at the source energy. Unlike the 14.1 MeV neutron source, the energy deposited for 2 MeV exceeds the total energy of the neutron, which is entirely nonphysical. The low energy depositions behave as expected.

The results of the 500 keV neutron source MCNP simulation detector responses with the F8 tally are shown in Figure **?** for the LBE RSM. The detector response curves have much lower values than the HDPE at this energy.

The 500 keV detector response shows similar traits to the 2 MeV detector response. The maximum pulse energy is near 700 keV, which is outside of the range for 500 keV neutrons. At lower energies, the increasing counts is not as apparent. The low counts at low energies may be attributed to the sparsity of bins at these enegies.

Fig. 5. Detector Response Energy Spectrum for 500 MeV Neutrons in LBE RSM.

B. Detector Response Functions

The detector response functions over the $2\pi\ \theta$ range are integrated detector responses over energy. The total counts in the bin represent the entire pulse count that is seen by the detector. This results of this section and the subsequent sections should be taken with the results of the energy depended detector responses in mind. Figure **??** shows the detector response function for the LBE RSM.

Fig. 6. LBE Response Function.

The LBE results determine that the RSM geometry has a four-fold degeneracy in total counts. The angular range of the peaks cooresponds very similarly to the angle range of the XY plane slice at a Z of 10 cm from Figure **??**. In practice, the whole detector response function is taken and compared to a library of repsonse functions, so this degeneracy is not limiting the capability wholly.

There are varying trends in the response based on the material length. Where width is largest, the 14.1 MeV neutrons have a peak pulse count. The 14.1 MeV neutrons are more penetrating and are able to reach the detector. The 500 keV neutrons have a peak pulse count where the thickness is minimum. Lower energy neutrons have a larger cross section, so the flux that reaches the detector has a large probability of interacting.

The results for the HPDE RSM are shown in Figure **??**. The HDPE pulse counts are in general less than for the LBE mask. It is important to note here that there is an appreciable amount of variability of the integrated response functions, which can allow for detection if enough data is taken for all of the potential outcomes based on source energy and direction.

Fig. 7. HDPE Response Function.

The results fo the HDPE RSM show the same trends as for the LBE RSM with the major exception of the 500 keV source neutrons and the magnitude of the counts in the detector. HDPE is composed of lighter atomic nuclei, which strongly perturbs the interaction of neutrons. Thermalization of neutron energies occurs as neutrons pass through the light material, which increases the cross section.

In the 500 keV case, the energy is thermalized enough that the neutrons are absorbed by the HDPE before they reach the detector. In the case of 14.1 and 2 MeV neutrons, the counts are generally lower than the LBE RSM. The 2 MeV neutrons have a larger than expected count rate in the thicker regions.

C. MAC Results

The results of the detector responses are complied into a MAC matrix. The MAC matrix compares each of the energy dependent responses against one another for a given material and neutron source energy.

The MAC matrix for 14.1 MeV neutrons in LBE is shown in Figure **??**. The other MAC matrices are not shown. The 500 keV HPDE RSM MAC matrix is not statistically significant, and the remaining MAC matrices behave nearly identically in magnitude and behavior to the 14.1 MeV is LBE.

Fig. 8. MAC Matrix for 14.1 MeV Neutrons in LBE RSM.

The MAC matrix shows nearly complete degeneracy in all of the values, which is expected from the relative shapes of the energy distributions in the pulse counts. There is a wide band that appears in each of the MAC matrices from bins of approximately 35 to 52. The bin range corresponds to a degree bin range of 175 to 260 degrees. The region that aligns with the degree bin range is that which has the greatest pulse count, with some extension. The results of each MAC matrix are compiled in Table **??**.

TABLE I
AN EXAMPLE OF A TABLE

MAC	Average	Average Error
14.1 MeV LBE	0.998	0.015
2 MeV LBE	0.993	0.018
500 keV LBE	0.996	0.013
14.1 MeV HDPE	0.998	0.019
2 MeV HDPE	0.993	0.014
500 keV HDPE	0.950	0.177

The results of each MAC are nearly complete equivalence in all directions for each energy source and for the LBE or HDPE material. The 500 keV sample with the HDPE did not achieve statistically significant results, as the HDPE does an effective job of shielding lower energy neutrons. The average MAC for each setup is in the range of 0.99, which is not enough to indicate the direction of the source with accuracy.

V. CONCLUSIONS

The RSM geometry and material selection is not feasible for neutron imaging with the results. The evaluation of the MAC matrices indicates that LBE is a superior material for the primary reason of not shielding from lower energy neutrons. It is important to note that this study is a very small selection of the RSM. Other directions in the RSM may provide less degeneracy and more suitable MAC results.

The detector response functions are not completely degenerate. This allows for the possibility of taking data in a slice around the RSM and potentially backing out the source direction based on a library of detector responses. Source characterization is possible if enough data of all of the source position and energies are known. Utilizing a large sample size by rotating the RSM and taking new data is not a rapid process and should be attempted to be avoided.

Improvements to the RSM can be achieved to increase the MAC values. A low MAC value will allow for a rapid determination of the source of the neutrons. The energy spectrum is too similar to distinguish directionality, which causes the MAC values to move to unity. Improvements to the RSM include changes to the geometry and materials selection to alter the neutron energy spectrum.

Potential improvements to the geometry and materials should be aimed to have properties of the LBE and HDPE. A likely path for this is to have an other region composed of LBE with an inner thinner shield of HDPE. This setup would provide the RSM with capabilities of highly scattering with both high and low energy loss. The result of which will increase the detector counts and help to spread out the neutron spectrum.

Future analysis should address a few key pieces absent from this study. Different geometry and materials should be studies, to acquire the full picture of the RSM. A new figure of merit may become apparent when the neutron energy spectrum is changed. It is suspected that changing the spectrum will allow for the MAC to have continued use. An investigation of the tally used and outliers should be conducted, which was not accomplished in this study. Finally, the simulation can be conducted in MCNP-PoliMI or GEANT to handle the particle interaction and tracking at a more fine level of detail. Documentation of this study is available on a Github Repository [**?**].

REFERENCES

[1] J. V. Logan, "Rotating Scatter Mask for Gamma Source Imaging," M.S. thesis, AFIT/ENP, Wright Patterson AFB, OH, 2017
[2] Robert Olesen. (2017) Rotating Scattering Mask Gamma MCNP Drill input. Available: https://github.com/nickquartemont/Neutron_RSM
[3] James E Bevins. (25 April 2017) Slaybaugh Lab 88 Data. Available: https://github.com/SlaybaughLab/88_Data/blob/master/Simulated/PHS/33MeVTa/BeamOnly/Model/33MeVTaBeamOnly_Det.i
[4] MCNP6 Users Manual, Los Alamos National Laboratory, Los Alamos, NM, USA, 2013.

[5] Handbook on Lead-bismuth Eutectic Alloy and Lead Properties, Materials Compatibility, Thermal-hydraulics and Technologies, 2007 ed., Nuclear Energy Agency, Paris, France, 2007, pp. 25-58.

[6] James E Bevins. (28 July 2017) MCNP.py. Available: https://github.com/jamesbevins/PyScripts/blob/master/src/GeneralNuclear/MCNP.py